American Journal of Engineering and Applied Sciences

Original Research Paper

The Study of the Dynamics of a Cebâşev Manipulator

Relly Victoria Virgil Petrescu

Department of Transport Traffic and Logistics, Traffic and Logistics, Transport, TTR, Bucharest Polytechnic University, Bucharest 060042 (CE) Romania, Romania

Article history
Received: 28-10-2022
Revised: 07-11-2022
Accepted: 15-11-2022

Email: rvvpetrescu@gmail.com

Abstract: The paper presents a new method for determining the dynamic parameters of a Cebâşev conveyor mechanism, solvable in two steps. In the first step, the classic method of preserving the kinetic energy of the entire mechanism is used to determine the rotating mass of the Cebâşev mechanism denoted by J*, this being the dynamic rotating mass of the entire mechanism reduced to the driving element 1 (of the crank type; classical rotating mass is called the mechanical or mass moment of inertia). In the second step (with the help of a new method), the dynamic angular speed of the Cebâşev mechanism's crank is directly determined, by using the mechanism's kinetic energy conservation a second time. This eliminates the need to use a more laborious classical method in the second step, such as differential Newton, Lagrange of type 1, Laplace transform, or Fourier, a finite difference method.

Keywords: Dynamics, Cebâşev Mechanism, Dynamic Rotating Mass of the Entire Mechanism Reduced to the Driving Element, Kinetic Energy Conservation

Introduction

A definition of dynamical physics or mechanics says that it is a branch of mechanics (see mechanical meaning 1) that deals with forces and their relationship primarily to motion, but sometimes to the equilibrium of bodies (Merriam-Webster, 2022). Dynamics is the discipline that deals with actual motion in any field, being the most important motion, which is why the study of dynamics in mechanics, as well as in other fields, is very important. Today, however, dynamics cover a multitude of aspects, starting from forces in systems and going to new technologies and technological processes. A methodology for the flexible implementation of collaborative robots in intelligent manufacturing systems is presented in the paper (Giberti *et al*., 2022). A robot arm design optimization method using a kinematic redundancy resolution technique is presented in (Maaroof *et al*., 2021). Trajectory control of industrial robots using multilayer neural networks driven by iterative learning control can be found in the paper (Chen and Wen, 2021). Dynamic and friction parameters of an industrial robot with repeatability identification, comparison and analysis are other important aspects of dynamic and robotic processes in the industry (Hao *et al*., 2021). The impact of gravity compensation on reinforcement learning in goal-setting tasks for robotic manipulators is a relatively new problem in dynamic disciplines (Fugal *et al*., 2021). Another dynamic new aspect is the mechatronic redesign of a manual assembly workstation in collaboration with wiring assemblies (Palomba *et al*., 2021), which can be directly associated with new technological processes.

Another aspect of the dynamic process appears in (Yamakawa *et al*., 2021) through the development of a high-speed, low-latency, remote-controlled robotic manual system. Accessible educational resources for teaching and learning robotics (Pozzi *et al*., 2021) is also a dynamic aspect, but different from the physical-mechanical one that is of particular interest to us in this study. Dynamic identification of the parameters of a pointing mechanism taking into account joint play (Sun *et al*., 2021) is a basic dynamic process. The impact of cycle time and payload of an industrial robot on resource efficiency (Stuhlenmiller *et al*., 2021) is also an important aspect of dynamic processes. Today, adaptive position (or force) control of a robot manipulator (Gierlak, 2021; Geng *et al*., 2021), as well as trajectory control (Colan *et al*., 2021; Liu *et al*., 2021; Engelbrecht *et al*., 2021; Alizade *et al*., 2021; Scalera *et al*., 2021), are important dynamic processes.

There is no need to discuss the importance of the articulated robots studied in this study because today they represent 90% of the industrial robots used almost everywhere, these articulated robots have the task of making practically all the components of a machine, moving and manipulating, or others having the role of processing. Industrial robots are automatic, programmable machines with multiple axes of motion that can move to perform a task. A motion axis is a joint in the robot body where a segment can move. For example, a three-axis robot can rotate at its base, move its arm up and down and rotate the handle at the end of the arm. They impress with their versatility, which allows them to be used in new types of application areas. Whether on the floor, ceiling, or wall-thanks to the integrated power supply and compact control system-such a well-established system offers maximum precision in the smallest spaces. The Safe-Robot functionality enables innovative automation concepts. Whether it is suitable for controlled atmosphere rooms, hazardous areas, hygienic or splash-proof design, it is always accurate and fast in every pattern and movement. Whether in dusty, wet, or sterile environments, such a robot achieves top performance in any production environment. Robots have penetrated everywhere, including the medical area and operating rooms (Petrescu *et al*., 2016). A special problem in the dynamic processes of robots (Petrescu and Petrescu, 2015 a-b, 2016, 2021) is the study of their kinematics, closely related to dynamics.

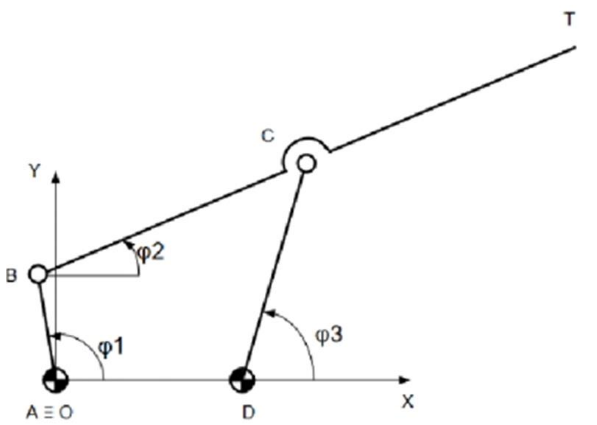

Fig. 1: A Cebâşev manipulator, (the plane part of the robot mechanism)

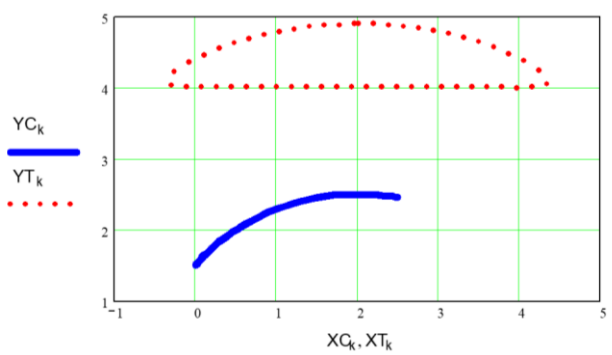

Fig. 2: In red one can see the trajectory of the T-end effector point of a Cebâşev manipulator, (the flat part of the robot mechanism)

Another important dynamic aspect (Essomba, 2021; Miguel-Tomé, 2021) is the balancing of technological processes. The influence of forces (Petrescu, 2022) is actually what determines the dynamic, real operation of all mechanical processes, including robots. In this way, it is possible to control the trajectory of robots and/or spacecraft (or drones) (Alpers, 2021; Caruso *et al*., 2021; Ebel *et al*., 2021; Thompson *et al*., 2021; Vatsal and Hoffman, 2021; Al Younes and Barczyk, 2021; Pacheco-Gutierrez *et al*., 2021; Stodola *et al*., 2021; Raviola *et al*., 2021; Medina and Hacohen, 2021; Malik *et al*., 2021).

The Cebasev manipulator robot (Fig. 1) described in the current work is a simple mechanism with planar movement, which can draw an almost straight line (Fig. 2) for a certain period of time with only one rotary motor that actuates the mobile element 1. AB, BT and DC are the length of the mobile elements 1, 2 and 3 and φ1 (or ϕ1), φ2, (or ϕ2) and φ3 (or ϕ3), are the angles that position the mobile elements in relation to the Ox axis.

This study will briefly present a new method for determining the dynamic parameters of the Cebâşev robot mechanism. The manipulator robot works in one plane (Fig. 1), but has a support (pivotal column) that supports it and can rotate it 360 degrees.

Methods

The centers of symmetry (of mass) of the three mobile elements are considered to be positioned according to Fig. 3, where element 2, the connecting rod, has its center of symmetry right in coupling C due to the constructive dimensions indicated by Cebâşev. S1, S2 (or C) and S3 represent the centers of symmetry of the three mobile elements belonging to the Cebâşev robot. m^1, m^2 and m^3 represent the masses of the three mobile elements each concentrated in the corresponding center of symmetry. JS1, JS2 (or JC) and JS3 represent the rotating masses of the three mobile elements considered each around the axis of rotation perpendicular to the plane of the robot in the corresponding center of symmetry.

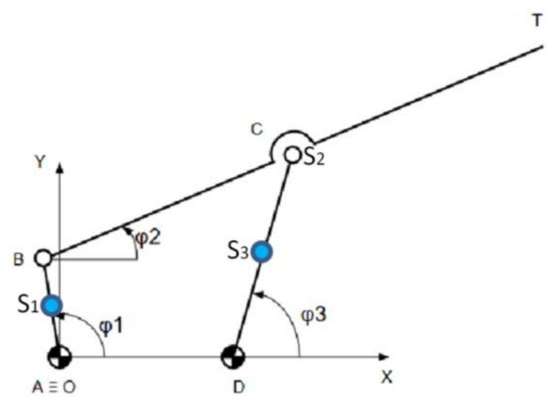

Fig. 3: The positioning of the centers of symmetry of the mobile elements belonging to the main Cebâşev mechanism

The initial relations of kinematic links between the kinematic elements of the mechanism, positions and speeds are established, to determine the speeds of mobile elements 2 and 3 depending on the known kinematic parameters of the first element, 1, driver (1-6):

$$\begin{cases} x_B = AB \cdot \cos\varphi_1 \\ y_B = AB \cdot \sin\varphi_1 \end{cases} \begin{cases} \dot{x}_B = -AB \cdot \sin\varphi_1 \cdot \dot{\varphi}_1 \\ \dot{y}_B = AB \cdot \cos\varphi_1 \cdot \dot{\varphi}_1 \end{cases} \tag{1}$$

$$\begin{cases} x_{S_1} = AS_1 \cdot \cos\varphi_1 \\ y_{S_1} = AS_1 \cdot \sin\varphi_1 \end{cases} \begin{cases} \dot{x}_{S_1} = -AS_1 \cdot \sin\varphi_1 \cdot \dot{\varphi}_1 \\ \dot{y}_{S_1} = AS_1 \cdot \cos\varphi_1 \cdot \dot{\varphi}_1 \end{cases} \tag{2}$$

$$\begin{cases} \begin{cases} x_{S_3} = x_D + DS_3 \cdot \cos\varphi_3 \\ y_{S_3} = y_D + DS_3 \cdot \sin\varphi_3 \end{cases} \\ \begin{cases} \dot{x}_{S_3} = \dot{x}_D - DS_3 \cdot \sin\varphi_3 \cdot \dot{\varphi}_3 = -DS_3 \cdot \sin\varphi_3 \cdot \dot{\varphi}_3 \\ \dot{y}_{S_3} = \dot{y}_D + DS_3 \cdot \cos\varphi_3 \cdot \dot{\varphi}_3 = DS_3 \cdot \cos\varphi_3 \cdot \dot{\varphi}_3 \end{cases} \end{cases} \tag{3}$$

$$\begin{cases} \begin{cases} x_C = x_D + DC \cdot \cos\varphi_3 \\ y_C = y_D + DC \cdot \sin\varphi_3 \end{cases} \\ \begin{cases} \dot{x}_C = \dot{x}_D - DC \cdot \sin\varphi_3 \cdot \dot{\varphi}_3 = -DC \cdot \sin\varphi_3 \cdot \dot{\varphi}_3 \\ \dot{y}_C = \dot{y}_D + DC \cdot \cos\varphi_3 \cdot \dot{\varphi}_3 = DC \cdot \cos\varphi_3 \cdot \dot{\varphi}_3 \end{cases} \end{cases} \tag{4}$$

$$\begin{cases} \begin{cases} x_C = x_B + BC \cdot \cos\varphi_2 \\ y_C = y_B + BC \cdot \sin\varphi_2 \end{cases} \\ \begin{cases} \dot{x}_C = \dot{x}_B - BC \cdot \sin\varphi_2 \cdot \dot{\varphi}_2 = -AB \cdot \sin\varphi_1 \cdot \dot{\varphi}_1 - BC \cdot \sin\varphi_2 \cdot \dot{\varphi}_2 \\ \dot{y}_C = \dot{y}_B + BC \cdot \cos\varphi_2 \cdot \dot{\varphi}_2 = AB \cdot \cos\varphi_1 \cdot \dot{\varphi}_1 + BC \cdot \cos\varphi_2 \cdot \dot{\varphi}_2 \end{cases} \end{cases} \tag{5}$$

Practically, system (6) solves the connection between the speeds of the three moving elements of the Cebâşev mechanism.

$$\begin{cases} -DC \cdot \sin\varphi_3 \cdot \dot{\varphi}_3 = -AB \cdot \sin\varphi_1 \cdot \dot{\varphi}_1 - BC \cdot \sin\varphi_2 \cdot \dot{\varphi}_2 \ | \cdot \cos\varphi_2 \ \| \cdot \cos\varphi_3 \\ DC \cdot \cos\varphi_3 \cdot \dot{\varphi}_3 = AB \cdot \cos\varphi_1 \cdot \dot{\varphi}_1 + BC \cdot \cos\varphi_2 \cdot \dot{\varphi}_2 \ | \cdot \sin\varphi_2 \ \| \cdot \sin\varphi_3 \\ \hline | \ DC \cdot \dot{\varphi}_3 \cdot \sin(\varphi_2 - \varphi_3) = AB \cdot \dot{\varphi}_1 \cdot \sin(\varphi_2 - \varphi_1) \Rightarrow \dfrac{\dot{\varphi}_3}{\dot{\varphi}_1} = \dfrac{AB}{DC} \cdot \dfrac{\sin(\varphi_2 - \varphi_1)}{\sin(\varphi_2 - \varphi_3)} \\ \| \ BC \cdot \dot{\varphi}_2 \cdot \sin(\varphi_2 - \varphi_3) = AB \cdot \dot{\varphi}_1 \cdot \sin(\varphi_3 - \varphi_1) \Rightarrow \dfrac{\dot{\varphi}_2}{\dot{\varphi}_1} = \dfrac{AB}{BC} \cdot \dfrac{\sin(\varphi_3 - \varphi_1)}{\sin(\varphi_2 - \varphi_3)} \end{cases} \tag{6}$$

Next, the kinetic energy conservation Eq. (7) is written on the entire mechanism for all mobile elements:

$$E_c = \frac{1}{2} J_{S_1} \cdot \dot{\varphi}_1^2 + \frac{m_1}{2} \cdot \left(\dot{x}_{S_1}^2 + \dot{y}_{S_1}^2\right) + \frac{1}{2} J_{S_2} \cdot \dot{\varphi}_2^2 + \frac{m_2}{2} \cdot \left(\dot{x}_{S_2}^2 + \dot{y}_{S_2}^2\right) + \frac{1}{2} J_{S_3} \cdot \dot{\varphi}_3^2 + \frac{m_3}{2} \cdot \left(\dot{x}_{S_3}^2 + \dot{y}_{S_3}^2\right) = const. \tag{7}$$

One then expresses twice the kinetic energy of the entire mechanism, which is also a constant (8):

$$2 \cdot E_c = J_{S_1} \cdot \dot{\varphi}_1^2 + m_1 \cdot \left(\dot{x}_{S_1}^2 + \dot{y}_{S_1}^2\right) + J_C \cdot \dot{\varphi}_2^2 + m_2 \cdot \left(\dot{x}_C^2 + \dot{y}_C^2\right) + J_{S_3} \cdot \dot{\varphi}_3^2 + m_3 \cdot \left(\dot{x}_{S_3}^2 + \dot{y}_{S_3}^2\right) = const. \tag{8}$$

The equation of conservation of double the kinetic energy of the entire mechanism is ordered (9):

$$2 \cdot E_c = J_{S_1} \cdot \dot{\varphi}_1^2 + J_C \cdot \dot{\varphi}_2^2 + J_{S_3} \cdot \dot{\varphi}_3^2 + m_1 \cdot \left(\dot{x}_{S_1}^2 + \dot{y}_{S_1}^2\right) + m_2 \cdot \left(\dot{x}_C^2 + \dot{y}_C^2\right) + m_3 \cdot \left(\dot{x}_{S_3}^2 + \dot{y}_{S_3}^2\right) \tag{9}$$

Then the previous equation is reduced to element 1 of the mechanism which is mobile and active (control and driving), by dividing the equation of twice the kinetic energy of the entire mechanism by the square of the angular velocity of crank 1 (10):

$$\frac{2 \cdot E_c}{\dot{\varphi}_1^2} = J_{S_1} + J_C \cdot \frac{\dot{\varphi}_2^2}{\dot{\varphi}_1^2} + J_{S_3} \cdot \frac{\dot{\varphi}_3^2}{\dot{\varphi}_1^2} + m_1 \cdot \frac{\left(\dot{x}_{S_1}^2 + \dot{y}_{S_1}^2\right)}{\dot{\varphi}_1^2} + m_2 \cdot \frac{\left(\dot{x}_C^2 + \dot{y}_C^2\right)}{\dot{\varphi}_1^2} + m_3 \cdot \frac{\left(\dot{x}_{S_3}^2 + \dot{y}_{S_3}^2\right)}{\dot{\varphi}_1^2} \tag{10}$$

After replacing the speeds written in the first equations, the double of the kinetic energy divided by the square of the angular speed of crank 1 takes the form (11):

$$\frac{2 \cdot E_c}{\dot{\varphi}_1^2} = J_{S_1} + J_C \cdot \frac{AB^2}{BC^2} \cdot \frac{\sin^2(\varphi_3 - \varphi_1)}{\sin^2(\varphi_2 - \varphi_3)} + J_{S_3} \cdot \frac{AB^2}{DC^2} \cdot \frac{\sin^2(\varphi_2 - \varphi_1)}{\sin^2(\varphi_2 - \varphi_3)} + m_1 \cdot AS_1^2 + m_2 \cdot AB^2 \cdot \frac{\sin^2(\varphi_2 - \varphi_1)}{\sin^2(\varphi_2 - \varphi_3)} + m_3 \cdot AB^2 \cdot \frac{DS_3^2}{DC^2} \frac{\sin^2(\varphi_2 - \varphi_1)}{\sin^2(\varphi_2 - \varphi_3)} \tag{11}$$

This equation is reduced to the simplified form (12):

$$\frac{2 \cdot E_c}{\dot{\varphi}_1^2} = J_{S_1} + m_1 \cdot AS_1^2 + J_C \cdot \frac{AB^2}{BC^2} \cdot \frac{\sin^2(\varphi_3 - \varphi_1)}{\sin^2(\varphi_2 - \varphi_3)} + \left(\frac{J_{S_3}}{DC^2} + m_2 + m_3 \cdot \frac{DS_3^2}{DC^2}\right) \cdot AB^2 \cdot \frac{\sin^2(\varphi_2 - \varphi_1)}{\sin^2(\varphi_2 - \varphi_3)} \tag{12}$$

In dynamic models it is known that the entire mechanism can be replaced with a single crank 1 whose rotating mass will take the form (13):

$$J^*_{1(S_1)} = \frac{2 \cdot E_c}{\dot{\varphi}_1^2} \tag{13}$$

or with a disc (or crack) with the center of rotation in coupling A, whose rotating mass will have the form (14):

$$J^*_{1(A)} = J^*_{1(S_1)} + AS_1^2 \cdot m_1 = \frac{2 \cdot E_c}{\dot{\varphi}_1^2} + AS_1^2 \cdot m_1 \tag{14}$$

To avoid the difficulties of using in step 2 the Lagrange equation of type 1 or 2 (as the case may be), the Newton equation in differential form, or the use of the Laplace or Fourier integral, or the use of other differential equations to linearize the system, will be used in following a simple, original, direct method, which also expresses the conservation of kinetic energy the second time and in this way it will be possible to directly determine the dynamic angular velocity of crank 1 and the corresponding dynamic angular acceleration, directly by deriving the already obtained dynamic angular velocity (15), (Petrescu, 2022):

$$\begin{cases} J_1^* \cdot \omega_1^{*2} = J_{1med}^* \cdot \omega_1^2 \Rightarrow \omega_1^* = \dfrac{\sqrt{J_{1med}^*}}{\sqrt{J_1^*}} \cdot \omega_1 \\ J_1^* = J_{1(A)}^*; \quad J_{1med}^* = J_{1(A)med}^* \\ \varepsilon_1^* = \omega_1^* \cdot \dfrac{d\omega_1^*}{d\varphi_1} \end{cases} \tag{15}$$

The values of the angular velocities of mobile elements 2 and 3 (16) can now be found immediately:

$$\begin{cases} \omega_2^* = \dfrac{AB}{BC} \cdot \dfrac{\sin(\varphi_3 - \varphi_1)}{\sin(\varphi_2 - \varphi_3)} \cdot \omega_1^* \\ \omega_3^* = \dfrac{AB}{DC} \cdot \dfrac{\sin(\varphi_2 - \varphi_1)}{\sin(\varphi_2 - \varphi_3)} \cdot \omega_1^* \end{cases} \tag{16}$$

To determine the reduced (dynamic) angular accelerations of mobile elements 2 and 3, the values of the kinematic angular velocities are replaced in the respective kinematic equations with the dynamic ones already obtained. Then the dynamic kinematics of the Cebâşev mechanism is determined, by using the old kinematic equations, in which both the angular velocities and the angular accelerations will be replaced with their dynamic values. The calculation program and the simulations performed in Mathcad can be found in the appendix.

Results

The mechanical (mass) moment of inertia of the entire mechanism reduced to crank 1 in coupling A can be traced in the diagram in Fig. 4. The dynamic angular velocities and dynamic angular accelerations of the three mobile elements can be traced in the diagrams of Fig. 5-10.

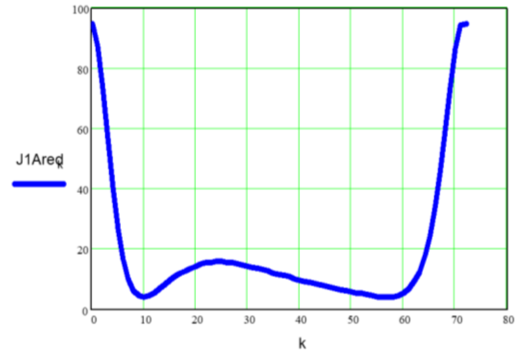

Fig. 4: The mechanical (mass) moment of inertia of the entire mechanism reduced to crank 1 in coupling A

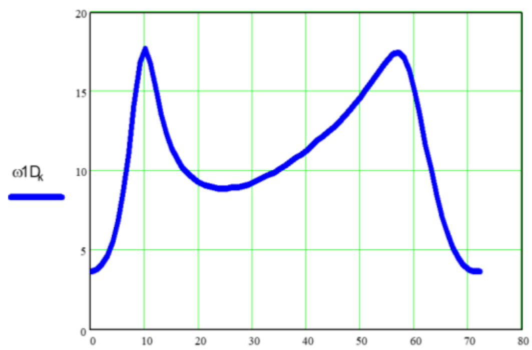

Fig. 5: The angular dynamic velocity of element 1

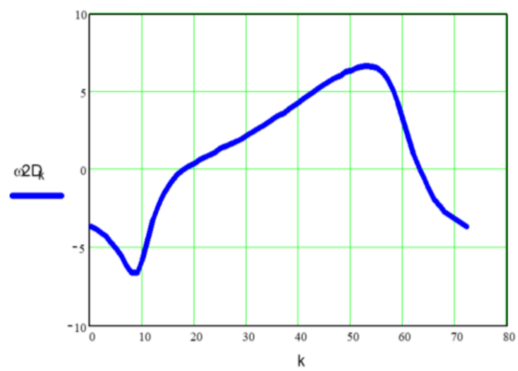

Fig. 6: The angular dynamic velocity of element 2

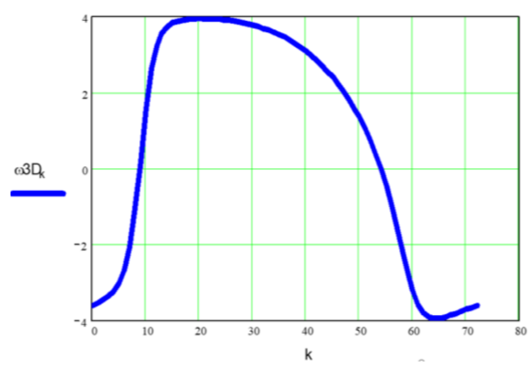

Fig. 7: The angular dynamic velocity of element 3

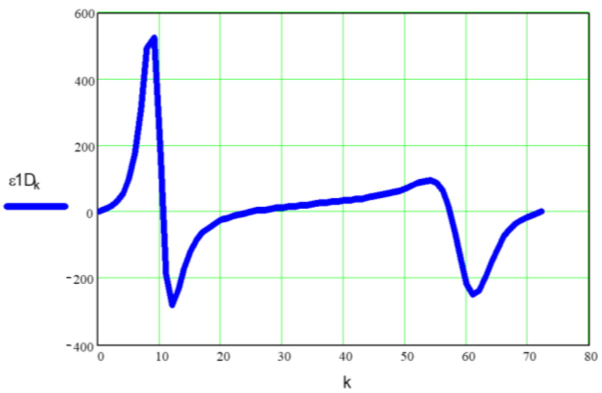

Fig. 8: The angular dynamic acceleration of element 1

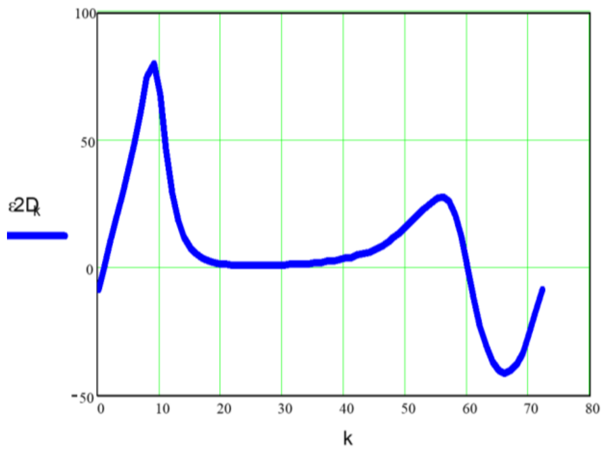

Fig. 9: The angular dynamic acceleration of element 2

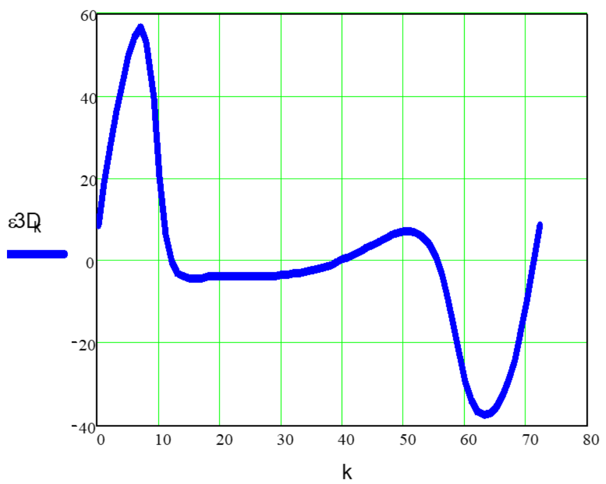

Fig. 10: The angular dynamic acceleration of element 3

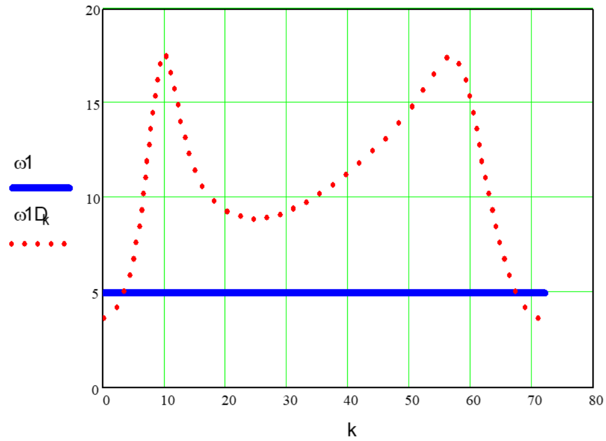

Fig. 11: Angular kinematic and dynamic velocities of the element 1

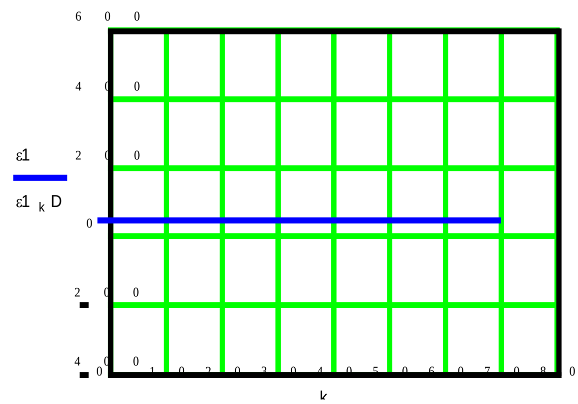

Fig. 12: Angular kinematic and dynamic accelerations of the element 1

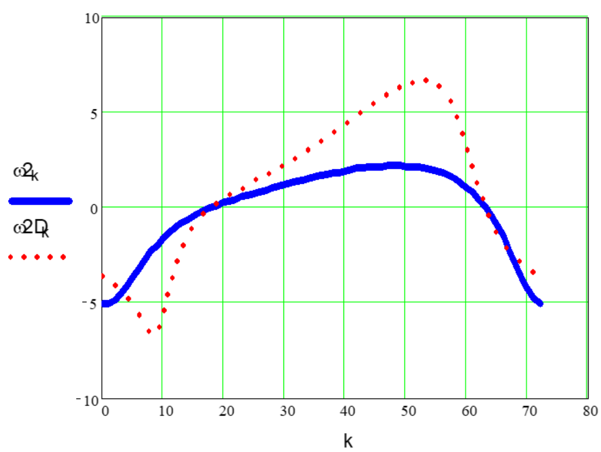

Fig. 13: Angular kinematic and dynamic velocities of the element 2

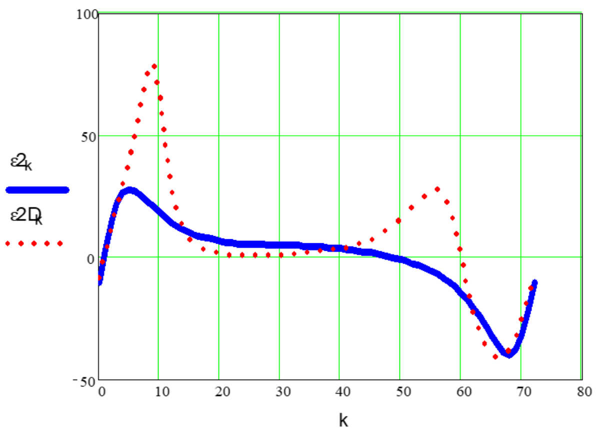

Fig. 14: Angular kinematic and dynamic accelerations of the element 2

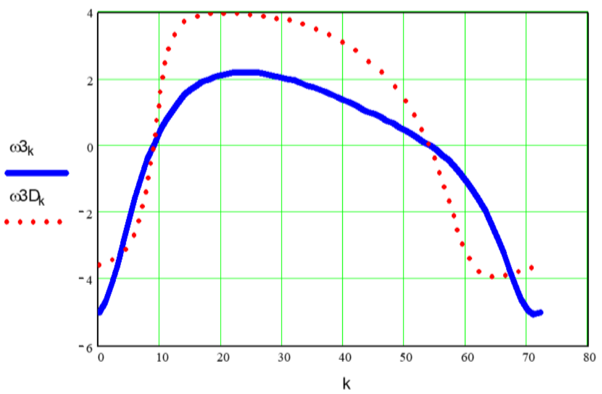

Fig. 15: Angular kinematic and dynamic velocities of the element 3

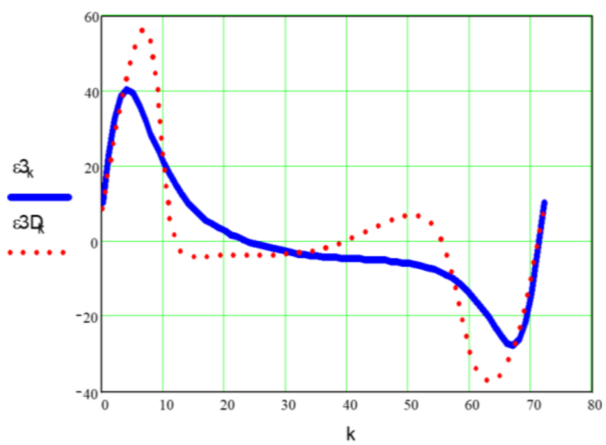

Fig. 16: Angular kinematic and dynamic accelerations of the element 3

For a comparative study between the kinematic and dynamic values, the diagrams in Fig. 11-16 were drawn.

All calculations and drawn diagrams can be found in the appendix. As you can see, the dynamics of the mechanism determined in two simple steps allows the calculation and plotting of the dynamic parameters very simply, in just two steps, the first being a classic one obtained by conservation of kinetic energy and the second step being a modern one where kinetic energy conservation is also used a second time (Petrescu, 2022), thus avoiding the need to use classical laborious methods, such as Newton's differential equations, the Lagrange equation of 1st order (for this mechanism), the Laplace transform or the Fourier integral, or various finite difference methods.

The method is simple to implement on any type of controller, a PID controller being simply designed and adapted thanks to this new method proposed in the current work, a method that can be generalized (Petrescu, 2022).

Discussion

Even if the presented dynamic method is the most general, the simple stand the most efficient, but also the fastest, it can be improved, because its dynamic effect is reduced to the inertial masses of the elements (both translation and rotation), introduced off the complete kinematic energies, during rotation and translation for each mobile element of the robot machine, these replacing the effect of the inertial forces in the mechanism on the real dynamic movement, without taking into account also the dynamic effects due to the links between the elements, i.e., the effects imposed by the kinematic couplings. For the introduction of these effects, it is necessary to correct the known, input angular speed,ω, with a dynamic factor D, by amplifying the rotating input speed with the dynamic factor D due to kinematic couples. In this type of mechanism (modular group), which contains two moving elements linked together by a kinematic coupling C5 (of the fifth class) of rotation, the dynamic coefficient D imposed by the mechanism has the value given by formula 17 (Petrescu, 2012).

$$D = \sin^2(\varphi_2 - \varphi_3) \tag{17}$$

The dynamic diagrams (noted with DD) after the correction applied by taking into account the dynamic coefficient D, which also represents the influence of the couples, have the forms (17-28).

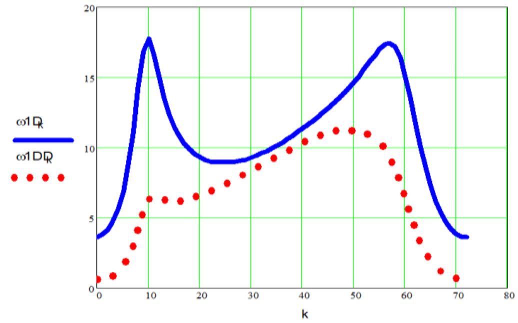

Fig. 17: The angular dynamic velocity of element 1

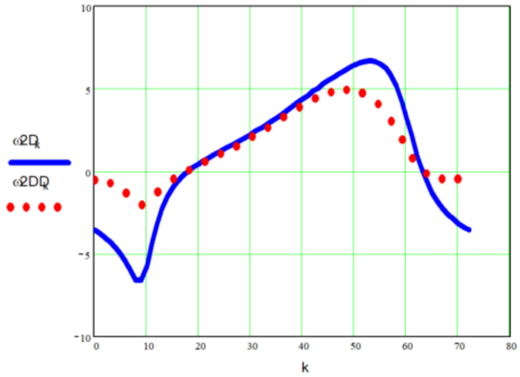

Fig. 18: The angular dynamic velocity of element 2

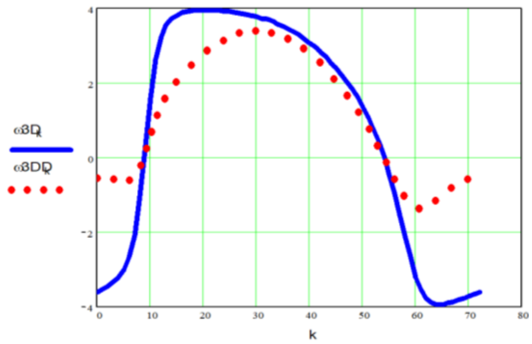

Fig. 19: The angular dynamic velocity of element 3

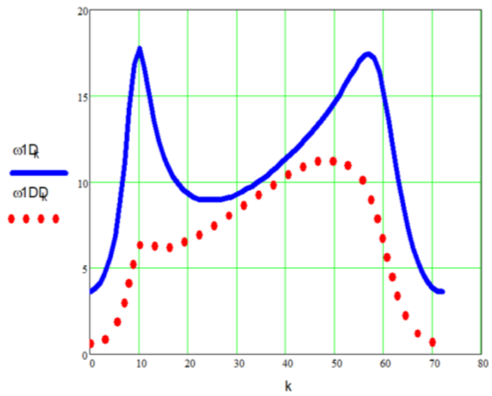

Fig. 20: The angular dynamic acceleration of element 1

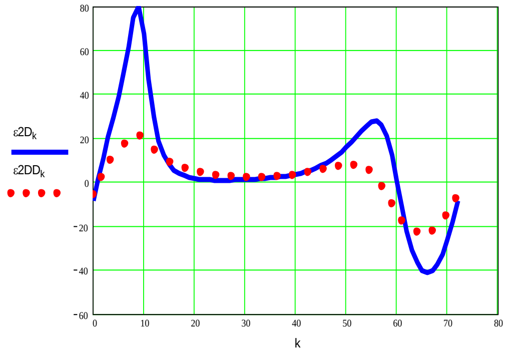

Fig. 21: The angular dynamic acceleration of element 2

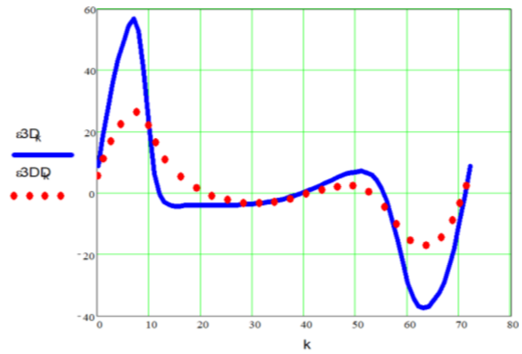

Fig. 22: The angular dynamic acceleration of element 3

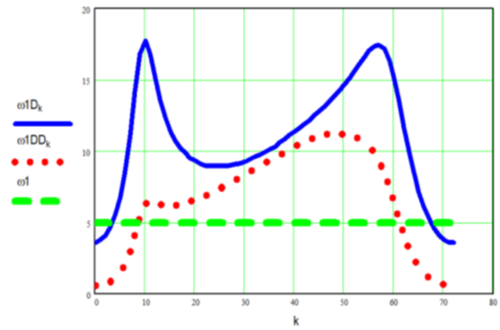

Fig. 23: Angular kinematic and dynamic velocities of the element 1

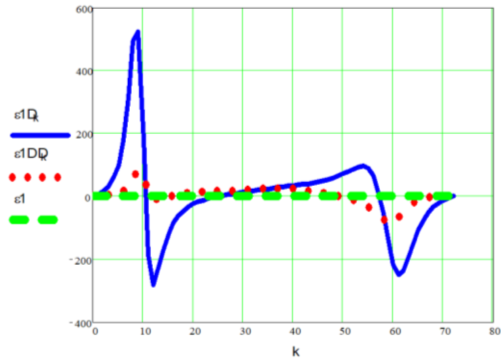

Fig. 24: Angular kinematic and dynamic accelerations of the element 1

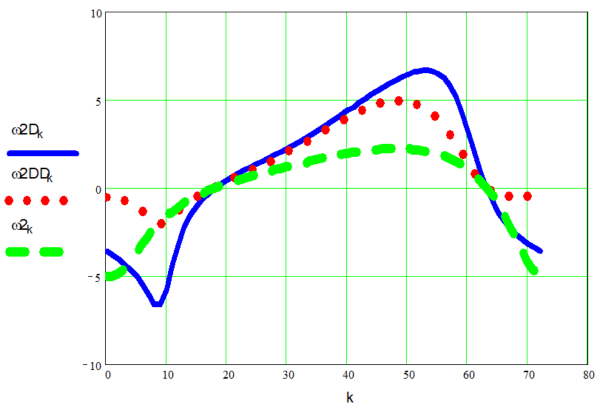

Fig. 25: Angular kinematic and dynamic velocities of the element 2

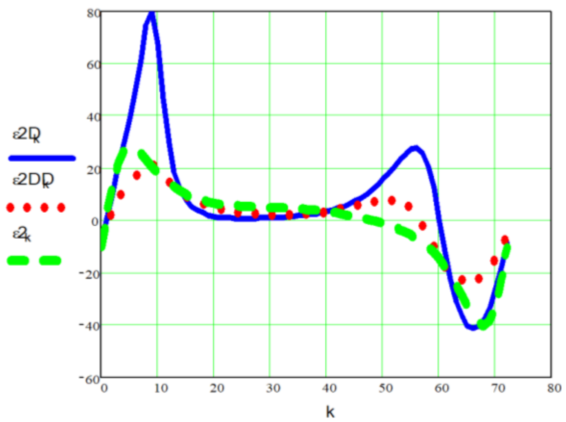

Fig. 26: Angular kinematic and dynamic accelerations of the element 2

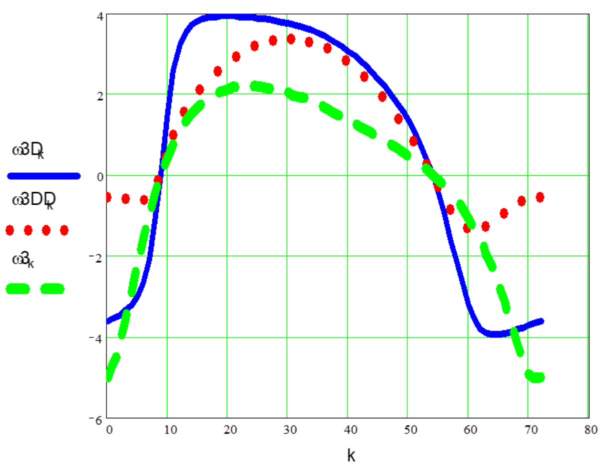

Fig. 27: Angular kinematic and dynamic velocities of the element 3

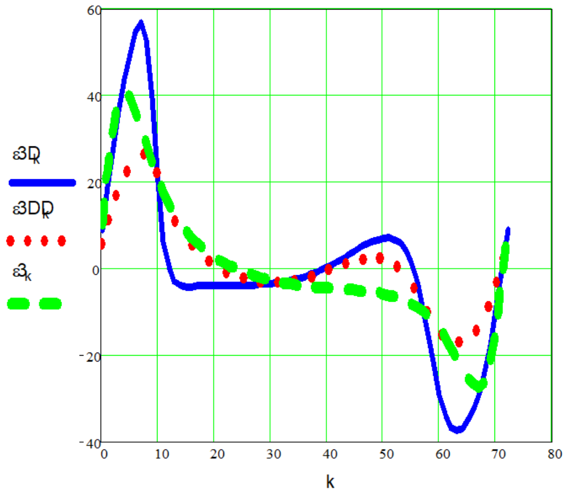

Fig. 28: Angular kinematic and dynamic accelerations of the element 3

For a comparative study between the kinematic and dynamic values, the diagrams in Fig. 23-28 were drawn.

It is easy to see that within the robot car, the couplings have a calming effect on the dynamic operation, reducing both the speeds and the angular accelerations of the mobile kinematic elements they connect.

All numerical simulations were performed with the help of the Mathcad program.

A professional method of determining the dynamic operation of a mechanism is a particular and laborious one, which determines the dynamics of a robot or a machine directly on the respective mechanism using its force diagram. Such a method, however, could only be presented separately, in another work.

Conclusion

The robot mechanism presented in the work is a pivoting column that supports and rotates at 360 degrees a Cebâşev planar robot.

The method is simple to implement on any type of controller, a PID controller being simply designed and adapted thanks to this new method proposed in the current work, a method that can be generalized.

As you can see, the dynamics of the mechanism determined in two simple steps allows the calculation and plotting of the dynamic parameters very simply, in just two steps, the first being a classic one obtained by conservation of kinetic energy and the second step being a modern one where kinetic energy conservation is also used a second time, thus avoiding the need to use classical laborious methods, such as Newton's differential equations, the Lagrange equation of 1st order (for this mechanism), the Laplace transform or the Fourier integral, or various finite difference methods.

The dynamic angular velocities and dynamic angular accelerations of the three mobile elements can be traced in the diagrams of Fig. 5-10.

For a comparative study between the kinematic and dynamic values, the diagrams in Fig. 11-16 were drawn.

A more precise dynamic study is also presented in which the influence of the kinematic couples that connect the mobile elements is also taken into account (Fig. 17-28).

Acknowledgment

This text was acknowledged and appreciated by Dr. Veturia CHIROIU Honorific member of the Technical Sciences Academy of Romania (ASTR) Ph.D. supervisor in Mechanical Engineering.

Funding Information

Research contract: Contract number 36-5-4D/1986 from 24IV1985, beneficiary CNST RO (Romanian National Center for Science and Technology) Improving dynamic mechanisms internal combustion engines.

Ethics

This article is original and contains unpublished material. The author declares that are no ethical issues and no conflict of interest that may arise after the publication of this manuscript.

References

Al Younes, Y., & Barczyk, M. (2021). Nonlinear model predictive horizon for optimal trajectory generation. *Robotics*, 10(3), 90. https://doi.org/10.3390/robotics10030090

Alizade, R., Soltanov, S., & Hamidov, A. (2021). Structural synthesis of lower-class robot manipulators with general constraint one. *Robotics*, 10(1), 14. https://doi.org/10.3390/robotics10010014

Alpers, B. (2021). On Fast Jerk-, Acceleration-and Velocity-Restricted Motion Functions for Online Trajectory Generation. *Robotics*, 10(1), 25. https://doi.org/10.3390/robotics10010025.

Caruso, M., Gallina, P., & Seriani, S. (2021). On the Modelling of Tethered Mobile Robots as Redundant Manipulators. *Robotics*, 10(2), 81. https://doi.org/10.3390/robotics10020081

Chen, S., & Wen, J. T. (2021). Industrial robot trajectory tracking control using multi-layer neural networks trained by iterative learning control. *Robotics*, 10(1), 50. https://doi.org/10.3390/robotics10010050

Colan, J., Nakanishi, J., Aoyama, T., & Hasegawa, Y. (2021). Optimization-based constrained trajectory generation for robot-assisted stitching in endonasal surgery. *Robotics*, 10(1), 27. https://doi.org/10.3390/robotics10010027

Ebel, L. C., Maaß, J., Zuther, P., & Sheikhi, S. (2021). Trajectory Extrapolation for Manual Robot Remote Welding. *Robotics*, 10(2), 77. https://doi.org/10.3390/robotics10020077

Engelbrecht, D., Steyn, N., & Djouani, K. (2021). Adaptive Virtual Impedance Control of a Mobile Multi-Robot System. *Robotics*, 10(1), 19. https://doi.org/10.3390/robotics10010019

Essomba, T. (2021). Design of a Five-Degrees of Freedom Statically Balanced Mechanism with Multi-Directional Functionality. *Robotics*, 10, 11. https://doi.org/10.3390/robotics10010011

Fugal, J., Bae, J., & Poonawala, H. A. (2021). On the impact of gravity compensation on reinforcement learning in goal-reaching tasks for robotic manipulators. *Robotics*, 10(1), 46. https://doi.org/10.3390/robotics10010046

Geng, J., Arakelian, V., Chablat, D., & Lemoine, P. (2021). Balancing of the Orthoglide taking into account its varying payload. *Robotics*, 10(1), 30. https://doi.org/10.3390/robotics10010030

Giberti, H., Abbattista, T., Carnevale, M., Giagu, L., & Cristini, F. (2022). A Methodology for Flexible Implementation of Collaborative Robots in Smart Manufacturing Systems. *Robotics*, 11(1), 9. https://doi.org/10.3390/robotics11010009

Gierlak, P. (2021). Adaptive position/force control of a robotic manipulator in contact with a flexible and uncertain environment. *Robotics*, 10(1), 32. https://doi.org/10.3390/robotics10010032

Hao, L., Pagani, R., Beschi, M., & Legnani, G. (2021). Dynamic and friction parameters of an industrial robot: Identification, comparison and repetitiveness analysis. *Robotics*, 10(1), 49. https://doi.org/10.3390/robotics10010049

Liu, R., Nageotte, F., Zanne, P., de Mathelin, M., & Dresp-Langley, B. (2021). Deep reinforcement learning for the control of robotic manipulation: A focussed mini-review. *Robotics*, 10(1), 22. https://doi.org/10.3390/robotics10010022

Maaroof, O. W., Dede, M. İ. C., & Aydin, L. (2021). A Robot Arm Design Optimization Method by Using a Kinematic Redundancy Resolution Technique. *Robotics*, 11(1), 1. https://doi.org/10.3390/robotics11010001

Malik, A., Henderson, T., & Prazenica, R. (2021). Multi-Objective Swarm Intelligence Trajectory Generation for a 7 Degree of Freedom Robotic Manipulator. *Robotics*, 10(4), 127. https://doi.org/10.3390/robotics10040127

Medina, O., & Hacohen, S. (2021). Overcoming Kinematic Singularities for Motion Control in a Caster Wheeled Omnidirectional Robot. *Robotics*, 10(4), 133. https://doi.org/10.3390/robotics10040133

Merriam-Webster. (2022). Definition of Dynamics (Entry 1 of 2); Merriam-Webster: 2022. Springfield, MA, USA. https://www.merriam-webster.com/dictionary/dynamics
Miguel-Tomé, S. (2021). The Heuristic of Directional Qualitative Semantic: A New Heuristic for Making Decisions about Spinning with Qualitative Reasoning. *Robotics*, 10(1), 17. https://doi.org/10.3390/robotics10010017
Petrescu, F. I. T. (2012). Theory of Mechanisms: Course and Applications, CreateSpace Independent Publishing Platform (September 12, 2012), Romanian Paperback: 286 pages, ISBN-13: 9781479302338.
Pacheco-Gutierrez, S., Niu, H., Caliskanelli, I., & Skilton, R. (2021). A Multiple Level-of-Detail 3D Data Transmission Approach for Low-Latency Remote Visualisation in Teleoperation Tasks. *Robotics*, 10(3), 89. https://doi.org/10.3390/robotics10030089
Palomba, I., Gualtieri, L., Rojas, R., Rauch, E., Vidoni, R., & Ghedin, A. (2021). Mechatronic re-design of a manual assembly workstation into a collaborative one for wire harness assemblies. *Robotics*, 10(1), 43. https://doi.org/10.3390/robotics10010043
Petrescu, F. I. T. (2022). Advanced Dynamics Processes Applied to an Articulated Robot. *Processes*, 10(4), 640. https://doi.org/10.3844/ajeassp.2022.59.80
Petrescu, F. I. T., & Petrescu, R. V. V. (2021). Direct kinematics of a manipulator with three mobilities. *Independent Journal of Management & Production*, 12(7), 1875-1900. https://doi.org/10.14807/ijmp.v12i7.1160
Petrescu, F. I., & Petrescu, R. V. (2015a). Forces at the main mechanism of a railbound forging manipulator. *Independent Journal of Management & Production*, 6(4). https://doi.org/10.14807/ijmp.v6i4.316
Petrescu, F. I., & Petrescu, R. V. (2015b). Kinematics at the main mechanism of a railbound forging manipulator. *Independent Journal of Management & Production*, 6(3). https://doi.org/10.14807/ijmp.v6i3.235
Petrescu, F. I., & Petrescu, R. V. (2016). Dynamic cinematic to a structure 2R. GEINTEC Journal, 6(2). https://ssrn.com/abstract=3074369
Petrescu, R. V., Aversa, R., Apicella, A., & Petrescu, F. I. (2016). Future medicine services robotics. American *Journal of Engineering and Applied Science*s, 9(4), 1062-1087. https://doi.org/10.3844/ajeassp.2016.1062.1087
Pozzi, M., Prattichizzo, D., & Malvezzi, M. (2021). Accessible educational resources for teaching and learning robotics. Robotics, 10(1), 38. https://doi.org/10.3390/robotics10010038
Raviola, A., Guida, R., De Martin, A., Pastorelli, S., Mauro, S., & Sorli, M. (2021). Effects of temperature and mounting configuration on the dynamic parameters identification of industrial robots. *Robotics*, 10(3), 83. https://doi.org/10.3390/robotics10030083
Scalera, L., Seriani, S., Gallina, P., Lentini, M., & Gasparetto, A. (2021). Human–robot interaction through eye tracking for artistic drawing. Robotics, 10(2), 54. https://doi.org/10.3390/robotics10020054
Stodola, M., Rajchl, M., Brablc, M., Frolík, S., & Křivánek, V. (2021). Maxwell Points of Dynamical Control Systems Based on Vertical Rolling Disc-Numerical Solutions. *Robotics*, 10(3), 88. https://doi.org/10.3390/robotics10030088
Stuhlenmiller, F., Weyand, S., Jungblut, J., Schebek, L., Clever, D., & Rinderknecht, S. (2021). Impact of Cycle Time and Payload of an Industrial Robot on Resource Efficiency. *Robotics*, 10(1), 33. https://doi.org/10.3390/robotics10010033
Sun, J., Han, X., Li, T., & Li, S. (2021). Dynamic Parameter Identification of a Pointing Mechanism Considering the Joint Clearance. *Robotics*, 10(1), 36. https://doi.org/10.3390/robotics10010036
Thompson, L. A., Badache, M., Brusamolin, J. A. R., Savadkoohi, M., Guise, J., Paiva, G. V. D., ...& Shetty, D. (2021). Multidirectional Overground Robotic Training Leads to Improvements in Balance in Older Adults. *Robotics*, 10(3), 101. https://doi.org/10.3390/robotics10030101
Vatsal, V., & Hoffman, G. (2021). The Wearable Robotic Forearm: Design and Predictive Control of a Collaborative Supernumerary Robot. *Robotics*, 10(3), 91. https://doi.org/10.3390/robotics10030091
Yamakawa, Y., Katsuki, Y., Watanabe, Y., & Ishikawa, M. (2021). Development of a high-speed, low-latency telemanipulated robot hand system. *Robotic*s, 10(1), 41. https://doi.org/10.3390/robotics10010041

Appendix

Establishing geometro-kinematic parameters:

XA	:	= 0
YA	:	= 0
BT	:	= 5
AB	:	= 1
BC	:	2.5
DC	:	2.5
XD	:	2
YD	:	= 0

Establishing the independent variable k and the entry angle FI1:

DOI: 10.3844/ajeassp.2022.239.254

K : = 0..72
$\phi 1k : = k$

Establishing the parameters of point B:

XB_k : = 0 + AB. cos ($\phi 1_k$)
XB_k : = 0 + AB. cos ($\phi 1_k$)
YB_k : = 0 + AB . sin ($\phi 1_k$)

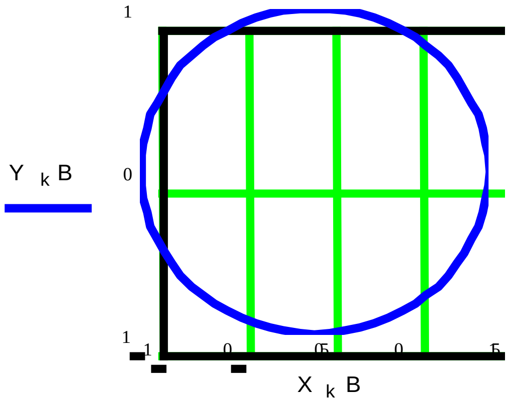

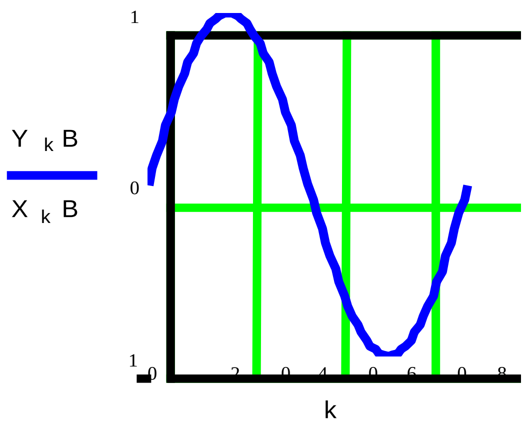

Establishing FI2 and FI3 parameters:

$\phi 20$:= 80
$\phi 2$:= $\phi 20$
$\phi 30$:= 115
$\phi 3$:= 30

Given

XB_k + BC. cos ($\phi 2$) = XD + DC. cos ($\phi 3$)
UB_k + BC. Sin($\phi 2$) = XD + DC. sin ($\phi 3$)

Sol_k : = Find ($\phi 2$, ϕ 3)

$$\begin{pmatrix} \phi 2_k \\ \phi 3_k \end{pmatrix} := sol_k$$

$$\begin{pmatrix} \phi 20_k \\ \phi 30_k \end{pmatrix} := sol_k \cdot \frac{180}{\pi}$$

Determining the parameters of points C and T:

XCk : = XBk + BC. cos ($\phi 2k$)
YCk : = YBk + BC. sin ($\phi 2k$)
XTk : = XBk + BT. cos ($\phi 2k$)
YTk : = YBk + BT. sin ($\phi 2k$)

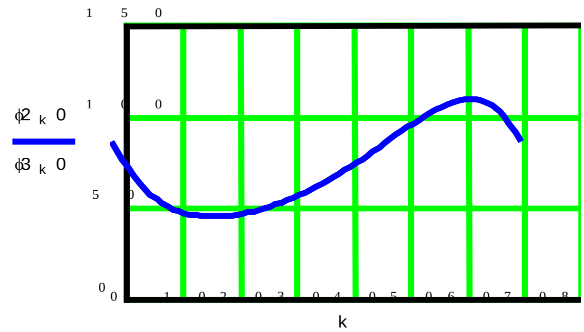

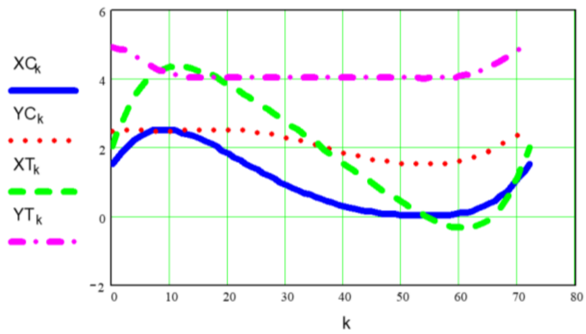

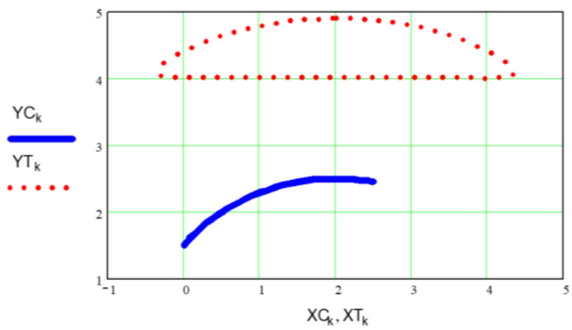

Determination of speeds and accelerations

$\omega 1$: = 5
XD1 : = 0
YD1 : = 0
$XB1_k$: = -AB . sin ($\phi 1_k$)$\cdot\omega 1$
$YB1_K$: = AB . cos ($\phi 1_k$)$\cdot\omega 1$
XD2 : = 0
$XB2_k$: = -AB . cos($\phi 1_k$)$\cdot\omega 1^2$
YD2 : = 0
$YB2_k$: =AB . sin ($\phi 1_k$)$\cdot\omega 1^2$

DOI: 10.3844/ajeassp.2022.239.254

$$\omega 2k := \frac{[(XB1k - XD1).\cos(\phi 3k) + (YB1_K - YD1).\sin(\phi 3_k)]}{BC.\sin(\phi 2_k - \phi 3_k)}$$

$$\omega 3k := \frac{[(XB1_k - XD1).\cos(\phi 2_k) + (YB1_K - YD1).\sin(\phi 2_k)]}{DC.\sin(\phi 2_k - \phi 3_k)}$$

$$\varepsilon 2k := \frac{(XB2_K - XD2).\cos(\phi 3_k) + (YB2_K - YD2).\sin(\phi 3_k) - (XB1_k - XD1).\sin(\phi 3_k).\omega 3_k - BC.\omega 2_K.\cos(\phi 2_k - \phi 3_k).(\omega 2_k - \omega 3_k)}{BC.\sin(\phi 2_k - \phi 3_k)}$$

$$\varepsilon 2k := \frac{(XB2_K - XD2).\cos(\phi 2_k) + (YB2_K - YD2).\sin(\phi 2_k) - (XB1_k - XD1).\sin(\phi 2_k).\omega 2_k + (YB1_K - YD1).\cos(\phi 2_K).\omega 2_k - DC.\omega 3_K.\cos(\phi 2_k - \phi 3_k).(\omega 2_k - \omega 3_k)}{DC.\sin(\phi 2_k - \phi 3_k)}$$

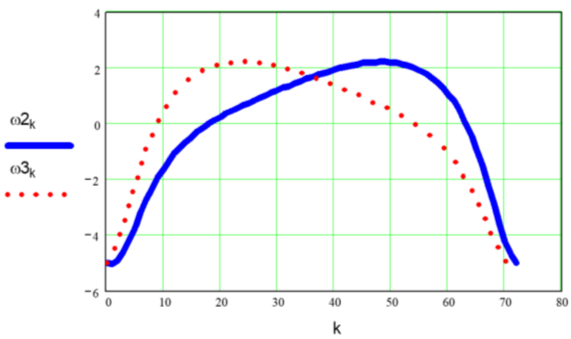

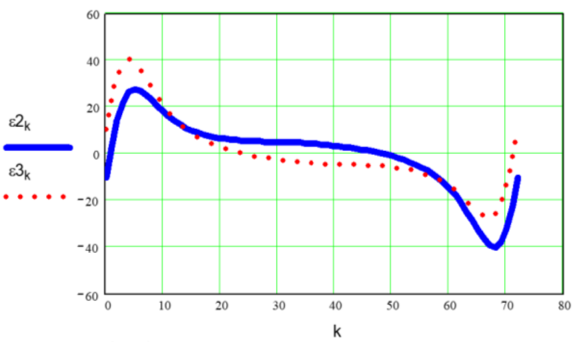

$XC1_k$: = $XB1_k - BC.\sin(\phi 2_k).\omega 2_k$
$YC1_k$: = $YB1_k + BC.\cos(\phi 2_k).\omega 2_k$

$$C1_K := \sqrt{(XC1_k)^2 + (YC1_k)^2}$$

$XC2_k$: = $XB2_k - BC.\cos(\phi 2_k).(\omega 2k)^2 - BC.\sin(\phi 2_k).\varepsilon 2_k$

$YC2_k$: = $YB2_k - BC.\sin(\phi 2_k).(\omega 2k)^2 + BC.\cos(\phi 2_k).\varepsilon 2_k$

$$C2_K := \sqrt{(XC1_k)^2 + (YC1_k)^2}$$

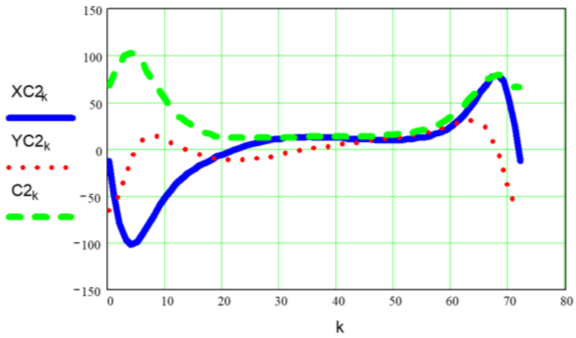

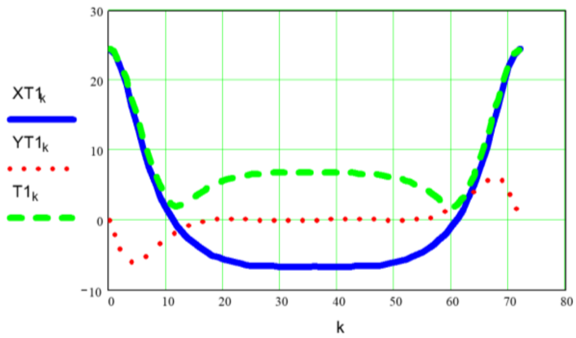

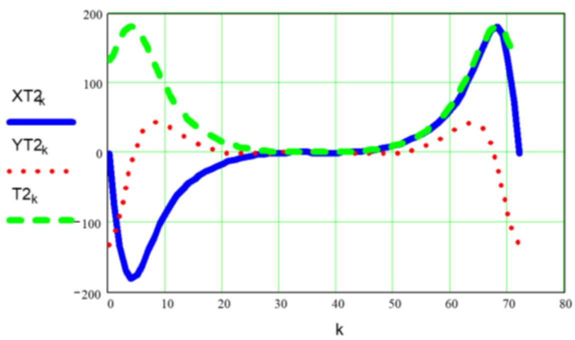

$XT1_k$: = $XB1_k - BT.\sin(\phi 2_k).\omega 2_k$
$YT1_k$: = $YB1_k + BT.\cos(\phi 2_k).\omega 2_k$

$$T1_K := \sqrt{(XT1_k)^2 + (YT1_k)^2}$$

$XT2_k$: = $XB2_k - BT.\cos(\phi 2_k).(\omega 2k)^2 - BT.\sin(\phi 2_k).\varepsilon 2_k$

$YT2_k$: = $YB2_k - BT.\sin(\phi 2_k).(\omega 2k)^2 + BT.\cos(\phi 2_k).\varepsilon 2_k$

$$T2_K := \sqrt{(XT2_k)^2 + (YT2_k)^2}$$

Dynamics – Kinetostatics (means forces)

ε1 : = 0
m2 : = 2
m3 : = 2

DOI: 10.3844/ajeassp.2022.239.254

$$AS1 := \frac{AB}{2}$$

$\varepsilon 1 := 0$

M2 : = 2 . BT
M3 : = 2 . DC
M1 : = 2 . AB

$$AS1 := \frac{AB}{2}$$

$$DS3 := \frac{DC}{2}$$

$$JS3 := M3.\frac{DC^2}{12}$$

RT : = –200

$$JS1 := m1.\frac{AB^2}{12}$$

$$JS1 := m1.\frac{AB^2}{12}$$

JC : = JS2

$XS3_k$: $= XD + DS_3 . \cos(\phi 3_k)$
$YS3_k$: $= YD + DS3 . \sin(\phi 3_k)$
$XS31_k$: $= -DS3. \sin(\phi 3_k) . \omega 3_k$
$YS31_k$: $= DS3. \sin(\phi 3_k) . \omega 3_k$
$XS32_k$: $= -DS3. \cos(\phi 3_k). (\omega 3_k)^2 - DS3 . \sin(\phi 3_k) . \varepsilon 3_k$

$YS32_k$: $= - DS3 . \cos(\phi 3_k) . (\omega 3_k)^2 + DS3 . \cos(\phi 3_k) . \varepsilon 3_k$

$XS1_k$: $= AS1. \cos(\phi 1_k)$
$YS1_k$: $= AS1. \sin(\phi 1_k)$
$XS11_k$: $= -AS1. \sin(\phi 1_k) . \omega 1$
$YS11_k$: $= AS1. \cos(\phi 1_k) . \omega 1$
$XS12_k$: $= -AS1 . \cos(\phi 1_k). \omega 1^2 - AS1. \sin(\phi 1_k). \varepsilon 1$
$YS12_k$: $= -AS1 . \sin(\phi 1_k). \omega 1^2 + AS1. \cos(\phi 1_k). \varepsilon 1$

$FixS1_k$: $= -m1 . XS12_k$
$FiyS1_k$: $= -m1 . YS12_k$
Mi1 : $= -JS1 . \varepsilon 1$

$$FiS1_K := \sqrt{(FiXS1_K)^2 + (FiyS1k)^2}$$

$FixS2_k$: $= -m2 . XC2_k$
$FiyS2_k$: $= -m2 . YC2_k$

$Mi2_k$: $= -JS2 . \varepsilon 2_k$

$$FiS2_K := \sqrt{(FiXS2_K)^2 + (FiyS2k)^2}$$

$FixS3_k$: $= -m3 . XS32_k$
$FiyS3_k$: $= -m3 . YS32_k$

$Mi3_k$: $= -JS3 . \varepsilon 3_k$

$$FiS3_K := \sqrt{(FiXS3_K)^2 + (FiyS3k)^2}$$

a11k : $= YC_k - YB_k$

$a12_k$: $= XB_k - XC_k$

$a1_k$: $= -Mi2_k + RT . (XC_k - XT_k)$

$a2_k$: $= FixS2_k. (YCk - YD) + FiyS2_k. (XD - XCk) - Mi2_k + RT. (XD - XT_k) + FixS3_k. (XD - XS3_k) - mi3_k$

$a21_k$: $= YD - YB_k$
$a22_k$: $= XB_k - XD$

Δx_k : $= a1_k . a22_k - a12_k. a2_k$
Δy_k : $= a11_k . a2_k - a1_k. a21_k$
Δ_k : $= a11_k . a22_k - a12_k. a21_k$

$$RBX_K := \frac{\Delta X_k}{\Delta_k}$$

$$RBy_K := \frac{\Delta y_k}{\Delta_k}$$

$$RBy_K := \sqrt{(RBX_k)^2 + (RBy_k)^2}$$

RDx_k : $= -(RBx_k + FixS2_k + FixS3_k)$
RDy_k : $= -(RBy_k + FiyS2_k + FiyS3_k + RT)$

$$RD_K := \sqrt{(RDX_k)^2 + (RDy_k)^2}$$

RCx_k : $= -(RBX_k + FixS2_k)$
RCy_k : $= -(RBy_k + FiyS2_k + RT)$

$$RC_K := \sqrt{(RCX_k)^2 + (RCy_k)^2}$$

$Mm1_k$: $= RBX_k. (YA - YB_k) + RBy_k. (XB_k - XA) - Mi1 + FixS1_k. (YS1_k - YA) + FiyS1_k. (XA - XS1_k$

RAX_k : $= RBX_k - FixS1_k$
RAy_k : $= RBX_k - FixS1_k$

$$RA_K := \sqrt{(RAX_k)^2 + (RAy_k)^2}$$

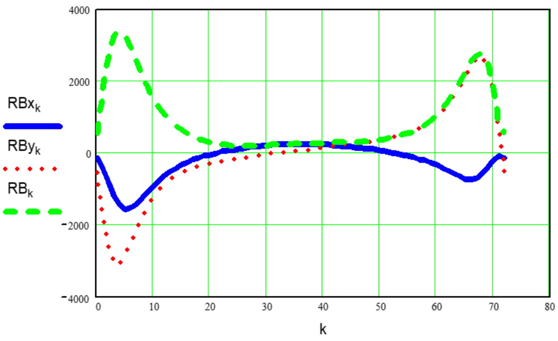

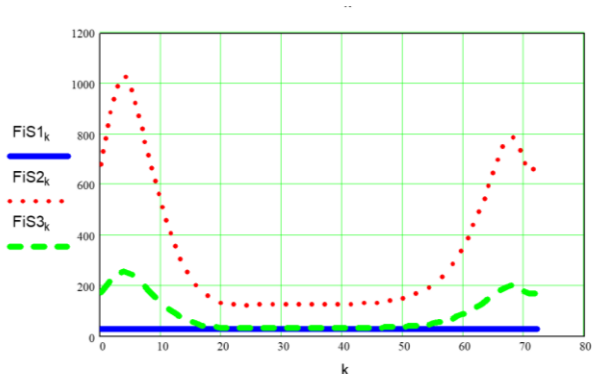

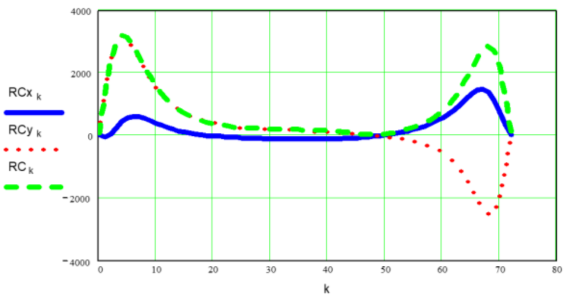

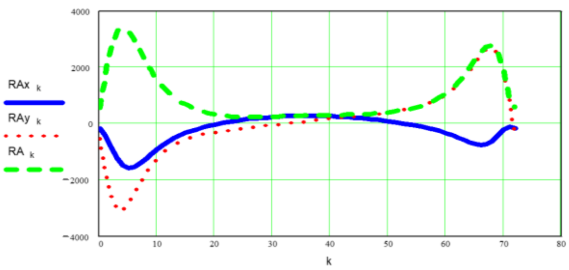

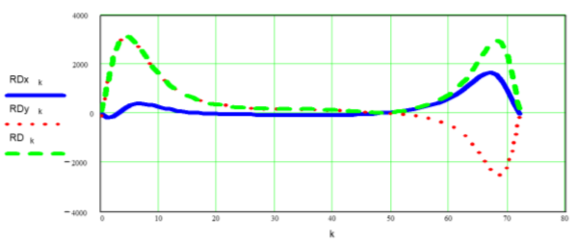

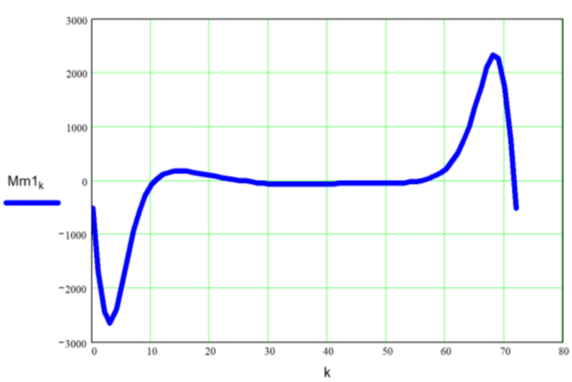

Dynamics - Dynamic Operation

$$J1Ared_k := JS1 + 2m1.AS1^2 + JC.\frac{AB^2}{BC^2}.\frac{(\sin(\phi3_k - \phi1_k))^2}{(\sin(\phi2_k - \phi3_k))^2} + \left(\frac{JC3}{DC^2} + m2 + m3.\frac{DS3^2}{DC^2}\right).AB^2.\frac{(\sin(\phi2k - \phi1_k))^2}{\sin(\phi2k - \phi3_k))^2}$$

$$\omega1D_k := \frac{\sqrt{\frac{(\max(J1Ared) + \min(J1Ared))}{2}}}{\sqrt{J1Ared_k}} \cdot \omega_1$$

$$\varepsilon1D_K := if\left[k < 1, 0, \omega1D_K.\frac{(\omega1D_k - \omega1D_{k-1})}{(\phi1_k - \phi1_{k-1})}\right]$$

$$\omega2D_K := \frac{AB}{BC}.\frac{\sin(\phi3_k - \phi1_k)}{\sin(\phi2_k - \phi3_k)}.\omega1D_K$$

$$\omega3D_K := \frac{AB}{DC}.\frac{\sin(\phi2_k - \phi1_k)}{\sin(\phi2_k - \phi3_k)}.\omega1D_K$$

$$\varepsilon2D_K := \frac{\left[\begin{array}{l}(XB2_k - XD2).\cos(\phi3_k) + (YB2_k - YD2).\sin(\phi3_k) - (XB1_k - XD1).\\ \sin(\phi3_k).\omega3D_k + (YB1_k - YD1).\cos(\phi3_k).\omega3D_k - BC.\omega2D_k.\cos(\phi2_k - \phi3_k).(\omega2D_k - \omega3D_k)\end{array}\right]}{BC.\sin(\phi2_k - \phi3_k)}$$

$$\varepsilon3D_K := \frac{\left[\begin{array}{l}(XB2_k - XD2).\cos(\phi2_k) + (YB2_k - YD2).\sin(\phi2_k) - (XB1_k - XD1).\sin(\phi2_k).\\ \omega3D_k + (YB1_k - YD1).\cos(\phi2_k).\omega2D_k - DC.\omega3D_k.\cos(\phi2_k - \phi3_k).(\omega2D_k - \omega3D_k)\end{array}\right]}{DC.\sin(\phi2_k - \phi3_k)}$$

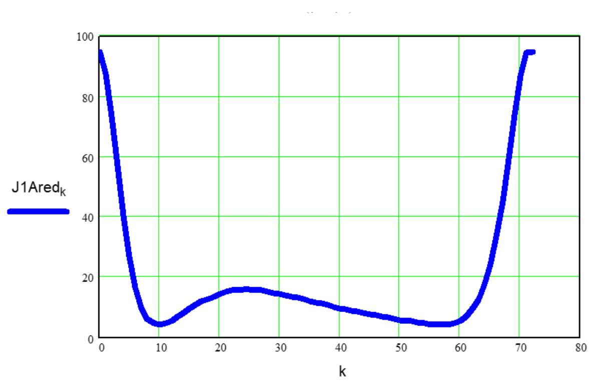

DOI: 10.3844/ajeassp.2022.239.254

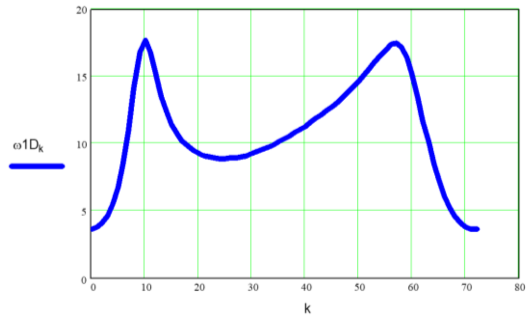

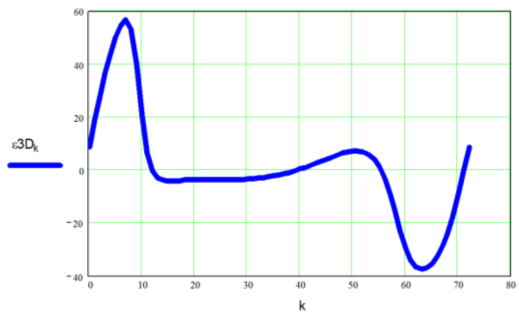

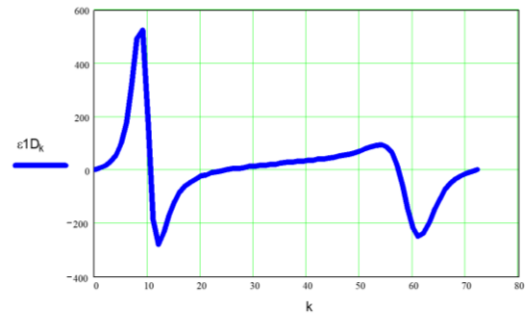

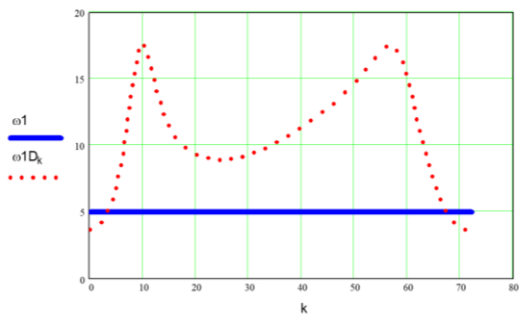

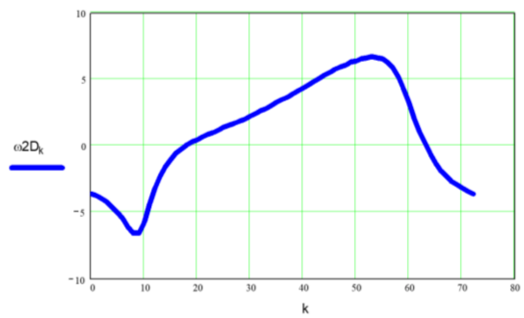

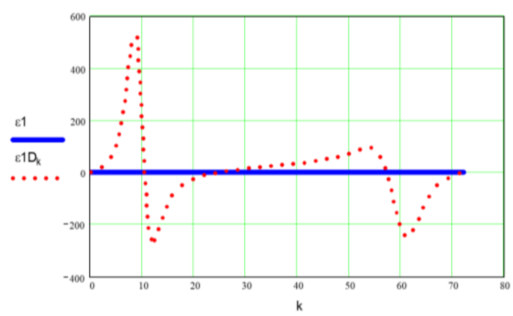

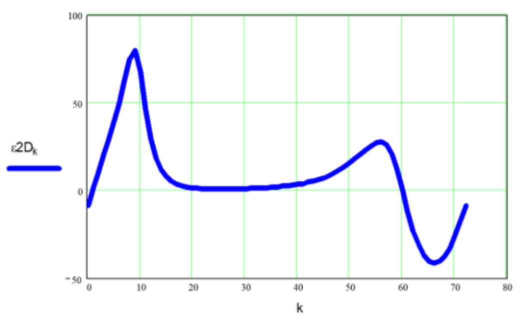

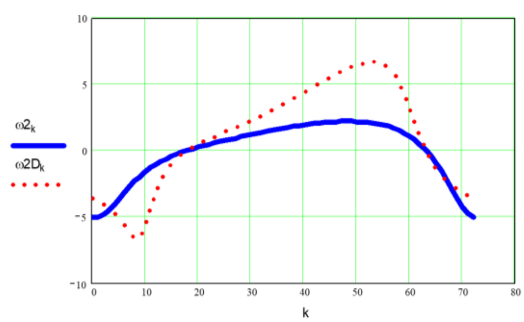

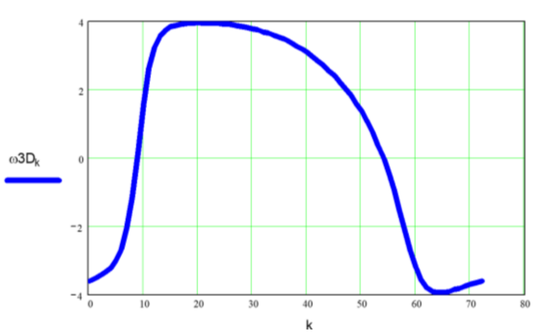

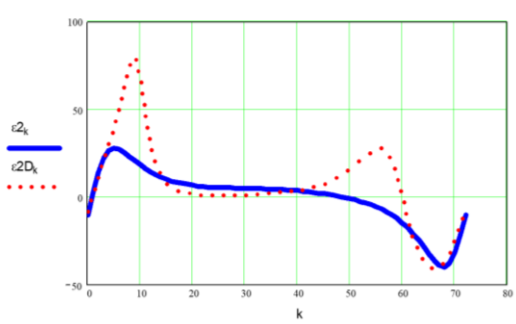

DOI: 10.3844/ajeassp.2022.239.254